DE GRUYTER Open Chem., 2018; 16: 745–756

Invited Paper Open Access

Richard Betz*

The structure of *ortho*-(trifluoromethyl)phenol in comparison to its homologues – A combined experimental and theoretical study

https://doi.org/10.1515/chem-2018-0066
received December 15, 2017; accepted April 17, 2018.

Abstract: The molecular and crystal structure of commercially-available *ortho*-(trifluoromethyl)phenol were determined by means of single-crystal X-ray diffractometry (XRD) and represent the first structural characterization of an *ortho*-substituted (trihalomethyl) phenol. The unexpected presence of a defined hydrate in the solid state was observed. Intermolecular contacts and hydrogen bonding were analyzed. The compound was further characterized by means of multi-nuclear nuclear magnetic resonance (NMR) spectroscopy (^{1}H, ^{13}C{^{1}H}, ^{19}F) and Fourier-Transform infrared (FT-IR) vibrational spectroscopy. To assess the bonding situation as well as potential reaction sites for reactions with nucleophiles and electrophiles in the compound by means of natural bonding orbital (NBO) analyses, and density functional theory (DFT) calculations were performed for the title compound as well as its homologous chlorine, bromine and iodine compounds. As far as possible, experimental data were correlated to DFT data.

Keywords: Phenols; NMR spectroscopy; X-ray structure determination; DFT calculations; NBO analysis.

1 Introduction

Phenol is among the simplest aromatic alcohols. The Brønstedt acidity of its hydroxyl group (pK_a = 9.89) [1] is significantly higher than that of common aliphatic alcohols such as methanol (pK_a = 15.5) or ethanol (pK_a = 15.9) [2] due to possible resonance stabilization of the corresponding alcoholate anion. As is observed for aliphatic alcohols whose acidity constants can be influenced by means of introducing electron-withdrawing and -donating functional groups on the hydrocarbon scaffold – *cf.* the pK_a values for 2-chloroethanol, 2,2-dichloroethanol and 2,2,2-trichloroethanol of 14.31, 12.89 and 12.24, respectively [2] – the Brønstedt acidity of phenol derivatives can also be fine-tuned by the presence of suitable substituents on the aromatic core [3]. In combination with the sterical pretense of the individual substituents or the plain substitution pattern on the aromatic core itself, this changed acidity can increase or decrease the bonding abilities of the respective aromatic alcohol's hydroxyl group in covalent and dative bonds. Upon variation of the substituents, derivatives of phenol, therefore, may be able to bind to a vast range of non- and (semi-)metals of the main group elements as well as transition metals in molecular and coordination compounds and give rise to interesting bonding patterns. For phenol and phenolate itself, ample structural information about its bonding behaviour – secured and elucidated on grounds of diffraction studies – is apparent in the literature and has shown phenolate to be a remarkably versatile bonding partner. It has been found to act as a strictly monodentate ligand towards main group and transition block elements such as, among others, beryllium [4], aluminium [5], gallium [6,7,8], tin [9], iron [10,11], osmium [12], uranium [13,14,15], neptunium [16], thorium [17], cobalt [18], zirconium [19], samarium [20], molybdenum [21] and tungsten [22,23] as well as a μ_2-bridging ligand towards, among others, lithium [24], aluminium [25], gallium [26], thallium [27], tantalum [28], tin [29], iron [30], titanium [31], copper [32] and mercury [33]. In addition, phenolate has further been confirmed to act as a μ_3-bridging ligand towards elements such as lithium [34] and zinc [35,36] and even as a μ_4-bridging ligand towards sodium [37]. Mixed mono- and bidentate bonding patterns supported by phenolate within one compound have also been reported for compounds based on sodium [38], barium [39], boron [40] and uranium [41]. Furthermore, phenolate has been found capable of acting simultaneously mono-, bi- and tri-dentate within

---

***Corresponding author: Richard Betz,** Nelson Mandela Metropolitan University, Summerstrand Campus (South), University Way, PO Box 77000, Port Elizabeth (Eastern Cape) 6031, South Africa, E-mail: Richard.Betz@nmmu.ac.za

one defined compound [42]. Intriguingly, phenol is also capable to act as a neutral as well as an anionic bonding partner simultaneously within one defined compound towards strontium [43] or titanium [44]. Motivated by this highly diverse chemical behaviour shown by plain phenol and phenolate, a research project aimed at elucidating the rules guiding the occurrence of specific bonding patterns in connection with the acidity as well as the steric pretense of substituents on the aromatic nucleus of phenol was initiated. As a starting point, *ortho*-(trifluoromethyl) phenol was chosen as it is a commercially-available compound that combines the presence of a strongly electron-withdrawing CF_3 group with its bulkiness in close proximity to the hydroxyl group that will act as the main reaction center. It was found that – as of today – structural information for *ortho*-methyl phenol or other *ortho*-CX_3-substituted (with X = F, Cl, Br and I) phenol derivatives is entirely absent from the literature thus precluding comparative studies with regards to the bonding patterns realized by the title compound and its inherent molecular metrical parameters. The only compounds featuring the *meta*-(trifluoromethyl)phenol moiety bonded to a heteroatom (i.e. no classical organic ethers) whose molecular and crystal structure have been elucidated on grounds of diffraction studies are found for a dinuclear titanium coordination compound [45] as well as two derivatives of phosphorus(V) [46]. Structural information about *para*-(trifluoromethyl)phenol-derived compounds with the latter moiety bonded to a heteroatom (i.e. no classical organic esters, ethers or oximes) is also scant and only available for two esters of phosphoric acid [47,48] as well as the symmetric ester of boronic acid [49]. A – purely theoretical – minor study about the hydrogen bonding situation and the conformational behaviour of the title compound has been reported earlier [50]. It is pertinent to note that no structural information at all is available in the literature for any derivatives of trichloromethyl-, tribromomethyl- or triiodomethyl-substituted phenols, regardless of the positioning of the halomethyl group on the aromatic core with respect to the hydroxyl group. A single-crystal X-ray analysis of the title compound was further deemed necessary to assess its chemical composition as a series of condensation and substitution reactions with hydrolytically-unstable substrates – where the title compound was used as one of the starting materials – yielded various hydrolysis products despite rigorously anhydrous working conditions. Preliminary infrared spectra recorded on macroscopic crystals of the title compound hinted on the presence of two different types of hydrogen bonds. Furthermore, due to the scant amount of information present in the literature for *ortho*-CX_3-substituted (with X = F, Cl, Br and I) phenol derivatives in general, DFT calculations were performed to assess the bonding situation in the title compound and its heavier homologues to allow for predictions about potential reaction sites for nucleophiles and electrophiles.

2 Experimental

2.1 Reagents, Instrumentation and Convention

ortho-(Trifluoromethyl)phenol was obtained from Fluorochem Ltd. Crystals suitable for the diffraction studies were obtained upon repeated sublimation of the compound at room temperature.

^{1}H and ^{13}C{^{1}H} NMR spectra were recorded in deuterochloroform on a Bruker Ultrashield 400 Plus spectrometer at 25°C at 400 MHz and 101 MHz, respectively, and are referenced to internal TMS or the solvent residual peak of the deuterated solvent [51].^{19}F NMR spectra were recorded on a Bruker Ultrashield 400 Plus spectrometer at 25°C at 377 MHz and are referenced to external $CFCl_3$. IR spectra were recorded on a Bruker Tensor 27 spectrometer equipped with a Bruker Platinum ATR unit.

While the calculations have been carried out on pure *ortho*-(trifluoromethyl)-phenol, all spectroscopic measurements in this study – i.e. each reference to the "title compound" – make use of the actual material that was found to represent a defined hydrate.

2.2 Spectral Data

^{1}H NMR (400 MHz, CDCl3, *d* / ppm): 7.56–7.51 (m, 1H, H_{ar}), 7.43–7.39 (m, 1H, H_{ar}), 7.03–6.94 (m, 2H, H_{ar}), 4.98 (broad, 1H, OH). ^{13}C NMR (100 MHz, CDCl3, *d* / ppm): 153.7 (d, *J* 2.0, C_{ar}), 133.6 (s, C_{ar}), 127.0 (q, *J* 5.1, C_{ar}), 124.3 (q, *J* 273, CF_3), 120.7 (s, C_{ar}), 117.7 (s, C_{ar}), 116.7 (q, *J* 29.9, C_{ar}). ^{19}F NMR (377 MHz, CDCl3, *d* / ppm): –61.1.

FT-IR (neat, n/cm^{-1}): 3342, 3333, 3176, 1616, 1603, 1513, 1461, 1355, 1320, 1254, 1223, 1209, 1170, 1107, 1055, 1034, 949, 861, 836, 789, 754, 647, 597, 549, 530, 470, 355.

2.3 DFT Calculations and NBO Analyses

The structure of the title compound as well as its homologues were optimized with Gaussian 09 [52] on the B3LYP/6-311++ G(2d,p) level of theory with an ultrafine

Table 1: Crystallographic data for the structure determination of the title compound.

Parameter **Chemical formula**	**Value** **4 ($C_7H_5F_3O$) × H_2O**
M_r (g mol^{-1})	666.46
Crystal system	Tetragonal
Spacegroup	$P4_2/n$
a (Å)	19.4264(6)
b (Å)	19.4264(6)
c (Å)	7.6508(2)
V (Å^3)	2887.30(19)
Z	4
ρ (g cm^{-3})	1.533
μ (mm^{-1})	0.155
Crystal size (mm)	0.526 × 0.502 × 0.318
θ-Range (°)	3.32–28.27
Reflections for metrics	9055
Absorption correction	Numerical
Transmission factors	0.8592–1.0000
Measured reflections	12980
Independent reflections	3521
R_{int}	0.0156
Mean σ(*I*)/*I*	0.0161
Reflections with *I* ≥2 σ (*I*)	2928
x, *y* (weighting scheme)	0.0413, 1.0109
Parameter	210
Restraints	0
$R(F_{obs})$	0.0407
$R_w(F^2)$	0.1054
S	1.049
Shift/error$_{max}$	0.001
Max. residual density (e Å^{-3})	0.222
Min. residual density (e Å^{-3})	−0.205

integration grid and very tight convergence criteria as singlet molecules under exclusion of symmetry in point group C_1 applying a solvent model for chloroform. The starting geometry was obtained by means of GaussView [53]. Frequency analyses were performed on the optimized structures to ensure that these represent minima on the global electronic potential hypersurface. Calculations of NMR shifts were conducted on the PBE1PBE/6-311++G(2d,p) level of theory using the gauge including atomic orbitals (GIAO) method [54] based on the optimized structures. A solvent model for chloroform was used in this step as well. The analysis and visualization of the molecular orbitals was conducted by the Avogadro [55] as well as the Chemcraft program suite [56]. For iodine, a pseudo-potential implemented in the LanL2DZ basis-set was applied throughout all calculations.

2.4 Crystallography

The diffraction studies on single crystals were performed at 200(2) K on a Bruker Kappa APEX-II CCD diffractometer (MoK_α, λ = 0.71073 Å). Structure solutions and refinement procedures were conducted by means of the SHELX program suite [57]. Crystallographic details of the structures are summarized in Table 1. Carbon-bound hydrogen atoms were calculated using the riding-model approximation and were included in the refinement with their U_H values set to 1.2U_{eq}(C). The hydrogen atom of the hydroxyl group was allowed to rotate with a fixed angle around the C–O bond to best fit the experimental electron density (HFIX 147 in the SHELX program suite), with *U*(H) set to 1.5 U_{eq}(C). The hydrogen atom of the water molecule was located on a difference Fourier map and was refined freely. Further details are provided in Table 1. Metrical parameters discussed for the crystal structure were obtained using PLATON [58], graphical presentations were prepared using Mercury [59] and ORTEP-III [60]. Crystallographic data of the title compound have been deposited with the Cambridge Structural Database (CCDC: 935348). Copies of the data can be obtained free of charge on application to the Director, CCDC, 12 Union Road, Cambridge CB2 1EZ, UK (Fax: int.code+(1223)336-033; e-mail for inquiry: file-server@ccdc.cam.ac.uk).

Ethical approval: The conducted research is not related to either human or animals use.

3 Results and Discussion

3.1 Crystal and Molecular Structure Analysis

The structure of the title compound is shown in Figure 1.

The asymmetric unit comprises two molecules of the aromatic compound as well as half a molecule of water on a special crystallographic position. Intramolecular C–C–C angles for both molecules cover a range of 119.06(13)–

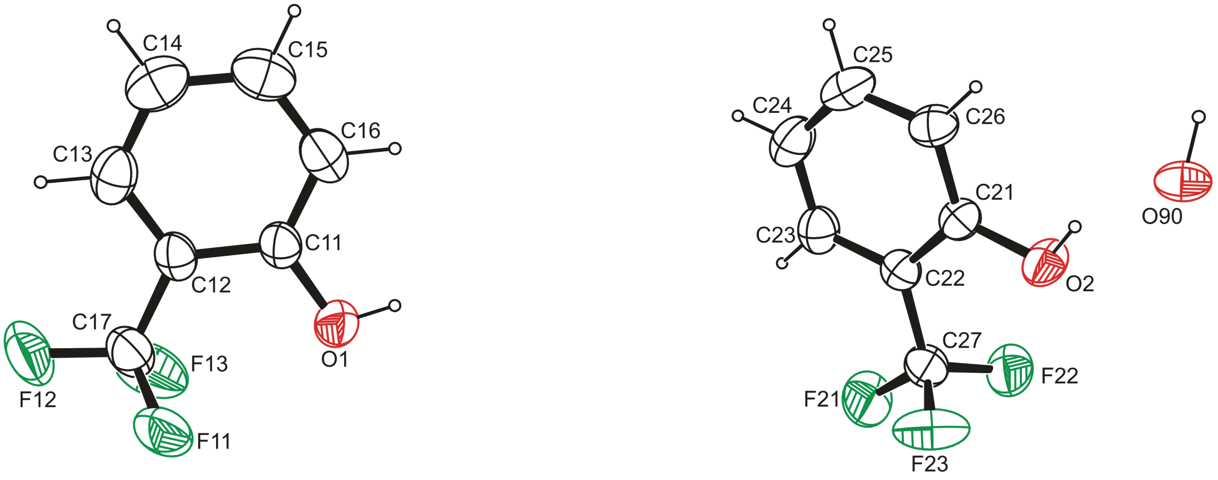

Figure 1: Molecular structure of the title compound, showing 50% probability displacement ellipsoids and atom labelling. Selected bond lengths (in Å): C11–C12 1.3971(17); C12–C17 1.489(2); C11–O1 1.3720(18); C21–C22 1.3924(17); C22–C27 1.4890(18); C21–O2 1.3605(15).

120.51(15)° and 119.51(13)– 121.03(13)°, respectively, with the largest angle invariably found on the carbon atom in *para* position to the trifluoromethyl-substituted carbon atom. In each molecule, the trifluoromethyl group adopts a staggered conformation with respect to the hydroxyl group. The least-squares planes defined by the respective carbon atoms of the two phenyl rings enclose an angle of 46.69(7)°. Selected bond lengths are given in the caption of Figure 1.

The two aromatic molecules in the asymmetric unit give rise to two different hydrogen bonding patterns completely independent from each other. While the first molecule forms isolated tetrameric units (Figure 2), the second molecule establishes – in connection with the water molecule present in the crystal structure – infinite chains along the crystallographic *c* axis (Figure 3).

In both patterns, cooperative hydrogen bonding is observed. Details about the hydrogen bonds are summarized in Table 2.

In terms of graph-set analysis [61,62], the descriptor for the hydrogen bonding pattern giving rise to the tetrameric units is $R^{4}_{4}(8)$ on the unary level while the infinite chains necessitate a *DD* descriptor on the same level. The shortest intercentroid distance between two aromatic systems was measured at 4.8077(9) Å in between the two different molecules present in the asymmetric unit and, therefore, rules out π-stacking to be a prominent stabilizing feature in the crystal.

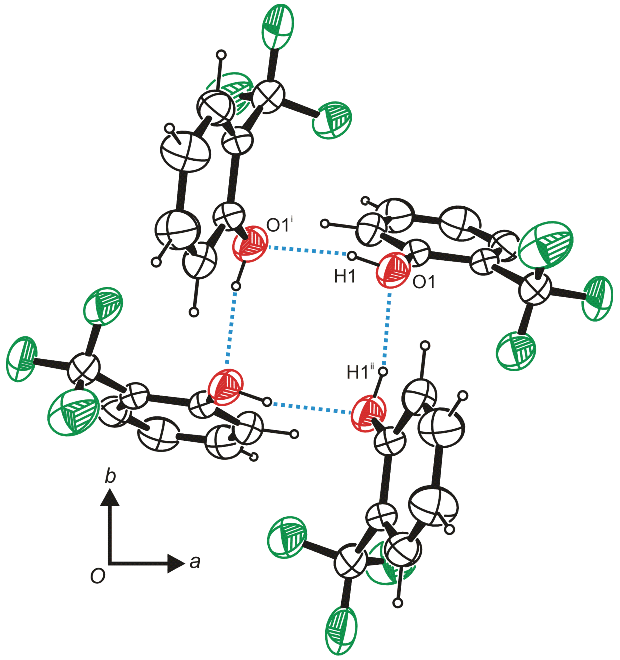

Figure 2: Cyclic tetrameric units in the crystal structure of the title compound, showing 50% probability displacement ellipsoids, viewed along [0 0 −1]. Symmetry operators: $^{\mathrm{i}}$ −y+1/2, x, −z+1/2; $^{\mathrm{ii}}$ y, −x+1/2, −z+1/2.

The crystal structure of the hydrate of non-substituted phenol has been described earlier and was found to feature chains – alternating between water molecules and phenol – along the crystallographic *c* axis [63]. However, no 3D coordinates have been deposited with the Cambridge Structural Database [64] to allow for a re-assessment of the situation at hand or comparative studies with regards to the title compound. A comparison of the hydrogen bonding situation encountered in the crystalline states of the title compound and water-free non-substituted phenol reveals an interesting picture. While a pseudo-helical chain-type connection along the crystallographic *a* axis of the three molecules present in the asymmetric

Table 2: Hydrogen bonds in the crystal structure of **1** (distances in Å, angles in °).

D	H	A	D–H	H...A	D...A	< D–H...A	Symmetry
O1	H1	O1	0.84	1.97	2.7957(15)	166.3	−y+1/2, x, −z+1/2
O2	H2	O90	0.84	1.89	2.6923(12)	158.5	
O90	H90	O2	0.874(18)	1.904(19)	2.7635(12)	167.7(18)	−y+1, x−1/2, z−1/2

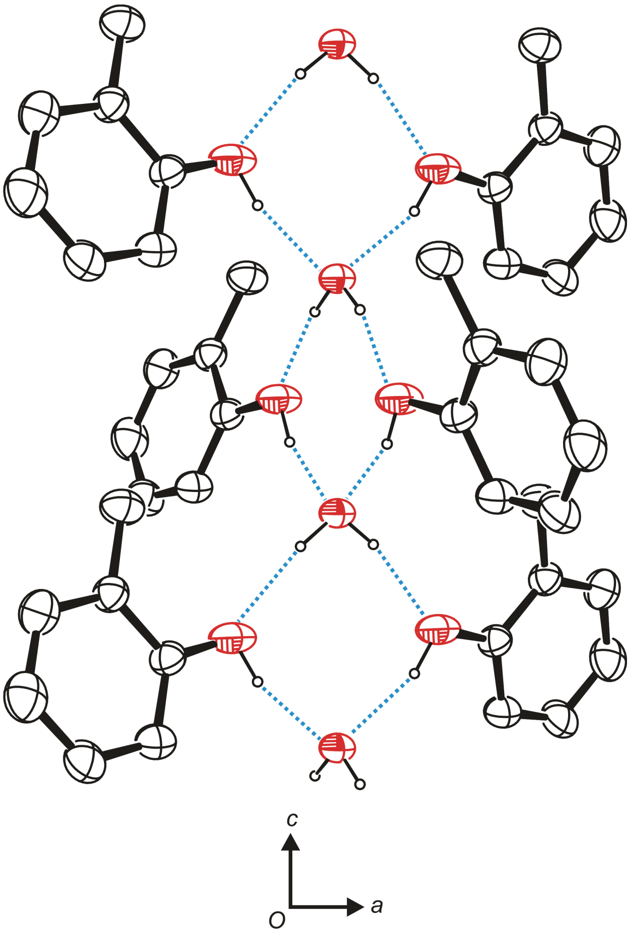

Figure 3: Infinite chains formed by hydrogen bonds in the crystal structure of the title compound, showing 50% probability displacement ellipsoids, viewed along [0 1 0]. For clarity, fluorine atoms as well as all carbon-bound hydrogen atoms were omitted.

unit of phenol was reported at ambient pressure [65], a slightly different situation is encountered in a high-pressure polymorph. In the latter case, two different chains – one exclusively made up of one of the three molecules present in the asymmetric unit, the other one alternately connecting the other two molecules present in the asymmetric unit – along the crystallographic *b* axis were reported [66]. The latter pattern as encountered in the high-pressure polymorph is, therefore, reminiscent of the chains supported by one of the two molecules of the title compound present in the asymmetric unit as well as the water molecule.

The lack of structural information available for comparable compounds in the literature precludes an in-depth comparable study about observable metrical trends with regards to the electronegativity of the halogen as well as the place of substitution.

3.2 Physical and Spectroscopic Properties

A proton NMR spectrum of the compound dissolved in dry deuterochloroform shows – apart from the expected set of aromatic protons – a broad signal around 4.9 ppm. The latter may be attributed to the phenolic hyxdroxyl group as well as the water molecule present in the title compound. ^{13}C NMR spectra show marked C-F coupling for the CF_3 group. The *ipso*-carbon atom as well as the two carbon atoms in *ortho* position to the trifluoromethyl group appear as quartets as well, however, C-F coupling is only weakly developed for the carbon atom bearing the hydroxyl group.

The presence of the different hydrogen bonding patterns in the title compound as established on grounds of the diffraction study based on single crystals is further corroborated by the results of vibrational spectroscopy as two neighbouring bands at 3441 and 3346 cm^{-1} are observed in the range that is typical for hydroxyl-groups. A splitting in this region of an IR spectrum has recently proven the presence of two distinguishable hydrogen bonds in case of the crystalline form of the cyanohydrine of cyclohexanone [67]. While the merging of the two bands in case of the latter compound was observed upon melting it close to room temperature, the same experiment could not be conducted for the title compound as the compound does not melt but rather sublimes at ambient conditions (see next paragraph).

Despite the extensive hydrogen bonding network, the compound is highly volatile. Even big crystals (~ 5 mm per edge) sublime completely within the course of a few hours if placed on a Petri-dish at ambient conditions.

Table 3: Comparison of selected (averaged) bond lengths (Å) and angles (°) for *ortho*-CX_3-substituted phenols (X = F, Cl, Br and I) calculated at the B3LYP/6-311++G(2d,p) level of theory (LanL2DZ in case of iodine) applying a solvent model for chloroform (DFT) with (averaged) experimental values for the fluorine derivative (XRD).

Bond lengths / Angles	F_{XRD}	F_{DFT}	Cl_{DFT}	Br_{DFT}	I_{DFT}
***d*(O–1)**	1.37	1.36	1.36	1.36	1.36
***d*(X–7)**	1.33	1.36	1.82	2.00	2.24
***d*(1–2)**	1.39	1.40	1.41	1.42	1.42
***d*(2–3)**	1.39	1.40	1.40	1.40	1.41
***d*(3–4)**	1.38	1.39	1.39	1.38	1.38
***d*(4–5)**	1.38	1.39	1.39	1.39	1.39
***d*(5–6)**	1.38	1.39	1.38	1.38	1.38
***d*(6–1)**	1.38	1.39	1.39	1.39	1.39
***d*(2–7)**	1.49	1.50	1.51	1.50	1.50
<(1–2–3)	119.4	119.6	118.1	117.6	116.6
<(2–3–4)	120.4	120.8	121.7	122.0	122.6
<(3–4–5)	119.8	119.3	119.5	119.6	119.7
<(4–5–6)	120.8	120.6	120.0	119.8	119.5
<(5–6–1)	119.8	120.4	120.9	121.0	121.1
<(6–1–2)	120.0	119.3	119.8	120.0	120.5

3.3 Quantumchemical Calculations

Due to the lack of experimental data available in the literature, it seemed of fundamental importance to assess the bonding situation and NMR characteristics as well as the metrical parameters of the title compound as well as its heavier homologues. Therefore, the structures of *ortho*-(trichloromethyl)phenol, *ortho*-(tribromomethyl) phenol and *ortho*-(triiodomethyl)phenol were modelled by DFT methods. As a benchmark, the title compound was subjected to the same DFT approach and the derived theoretical values were, as far as possible, correlated to experimental data. For all discussions, a labelling scheme as indicated in Figure 4 is used.

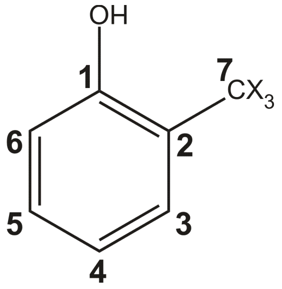

Figure 4: Labelling scheme applied for discussion of DFT results.

3.4 Metrical Parameters

In a first step, the metrical parameters were compared. The individual values for all calculated compounds are listed in Table 3.

As can readily be seen, the calculated values of the title compound show good agreement with the experimentally found ones thus proving the suitability of the chosen method and basis-set for the calculation. The slight differences in between these two kinds of values can be rationalized by taking into account packing effects in the crystal that are not accounted for by the DFT calculations applying a solvent model as well as the influence of the water molecule and its pertaining hydrogen bonding system present in the crystal structure might have. The C–O as well as the C–CX_3 bond lengths remain vastly unaffected by the nature of the halogen substituent present. While the intracyclic angles on the carbon atom bearing the CX_3 group as well as the carbon atom in *para* position to the latter gradually decrease with

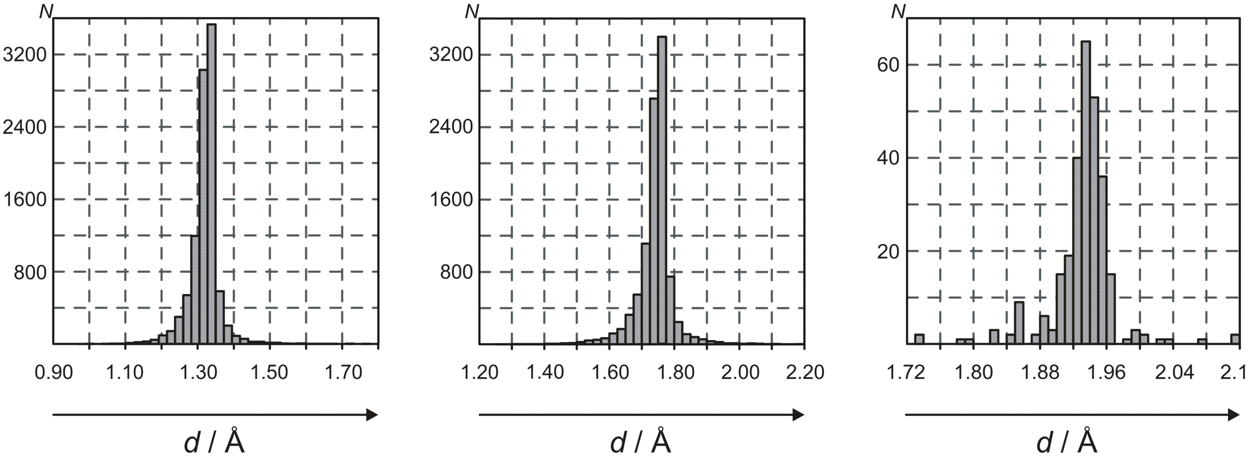

Figure 5: Distribution of C–X bond lengths for compounds featuring CX_3 moieties whose metrical parameters have been deposited with the Cambridge Structural Database [64] for CF_3 (left), CCl_3 (center) and CBr_3 (right) (CSD version 5.35, updates May 2014).

the increasing size of the halogen atoms present on the trihalomethyl moiety, all other intracyclic C–C–C angles invariably grow bigger at the same time. This trend can be explained by the increasing steric bulk of the respective CX_3 group with respect to the neighbouring hydroxyl group that will result in an increasing "pull" on the aromatic scaffold. As expected, the respective C–X bonds are getting longer with increasing size of the halogen. It is pertinent to note that the predicted (and, in case of fluorine, found) values are in good agreement with the most common values observed for the respective CX_3 groups in compounds whose metrical parameters have been deposited with the Cambridge Structural Database [64] (*cf.* Figure 5).

While ample structural information is available for compounds with CF_3 and CCl_3 groups, considerable less studies have been conducted for compounds containing CBr_3 substituents. For the heaviest moiety – CI_3 – only iodoform [68] or compounds classifying as co-crystallizates thereof have been reported, the only exceptions being tetraiodomethane [69] and an alkoxidoaluminate salt of the CI^{3+} cation [70].

3.5 NMR Parameters

In addition to the metrical parameters, carbon NMR shifts were calculated for the title compound as well as for its heavier homologues. An overview of the calculated (DFT) and experimentally-determined (EXP) shifts relative to tetramethylsilane (TMS) as a reference is given in Table 4. The labelling scheme given in Figure 4 is used to identify the individual carbon atoms.

The experimental ^{13}C NMR shifts for the CF_3-substituted phenol invariably are found at slightly higher fields than predicted. The deviation from the found values is most pronounced for the carbon atom of the CF_3 group as well as the carbon atom bearing the hydroxyl group. For all other carbon atoms the discrepancy between experimental and respective theoretical values is small and in the range of few parts per million. The theoretical data obtained will allow for an assignment of carbon resonances once the chlorine, bromine and iodine homologues of the title compound are accessible experimentally.

3.6 Natural Charges

To allow for the identification of preferred centers of reactivity of the title compound with regards to reactions with nucleophiles as well as electrophiles, the natural charges of the non-hydrogen atoms of the title compound as well as its heavier homologues were calculated. An overview of the numerical values for all four compounds is given in Table 5. The labelling scheme as outlined in Figure 4 is retained.

It can be seen that – apart from the carbon atom bearing the respective CX_3 group – the natural charges calculated for the carbon atoms of the aromatic system of the four different *ortho*-(trihalomethyl) phenols remain vastly unaffected by the nature of the halogen. The slight changes in the natural charge of the carbon atom bearing the CX_3 moiety can be explained as a superposition of the electronic situation encountered in the respective CX_3 unit as well as the change in the bonding distance between C2

Table 4: Comparison of ^{13}C NMR shifts for *ortho*-CX_3-substituted phenols (X = F, Cl, Br and I) calculated at the PBE1PBE/6-311++G(2d,p) level of theory (LanL2DZ in case of iodine) applying a solvent model for chloroform (DFT) with experimental values for the fluorine derivative (EXP). All values are given relative to TMS as the reference.

Atom	F_{EXP}	F_{DFT}	Cl_{DFT}	Br_{DFT}	I_{DFT}
C1	153.7	161.4	161.0	161.2	160.8
C2	116.8	119.3	132.9	137.2	143.2
C3	127.0	132.2	132.4	133.4	133.7
C4	120.7	124.3	123.5	123.2	122.6
C5	133.6	140.2	139.9	140.3	139.9
C6	117.6	122.6	123.6	123.8	123.7
C7	124.3	135.8	131.3	134.1	114.1

Table 5: Natural charges of the non-hydrogen atoms of *ortho*-CX_3-substituted phenols (X = F, Cl, Br and I) calculated at the B3LYP/6-311++G(2d,p) level of theory (LanL2DZ in case of iodine) applying a solvent model for chloroform (DFT). The labelling scheme as outlined in Figure 4 is used for the carbon atoms, 'X' refers to the respective halogen atoms whose charge has been averaged over all three atoms present in the CX_3 moiety.

Atom	F	Cl	Br	I
C1	+0.35	+0.35	+0.35	+0.35
C2	−0.23	−0.20	−0.22	−0.24
C3	−0.16	−0.16	−0.16	−0.16
C4	−0.24	−0.23	−0.23	−0.23
C5	−0.16	−0.16	−0.16	−0.16
C6	−0.24	−0.24	−0.24	−0.24
C7	+1.08	−0.13	−0.34	−0.67
O	−0.69	−0.69	−0.69	−0.69
X	−0.37	−0.03	+0.10	+0.23

and C7 (according to the labelling outlined in Figure 4). The biggest changes in the natural charge are observed within the various CX_3 groups. In accordance with the differences in electronegativity for carbon and the halogens according to Allen – C: 2.544, F: 4.193, Cl: 2.869, Br: 2.685, I: 2.359 [71] – the natural charge of the carbon atom of the CX_3 group changes from a markedly positive value in the case of fluorine to a negative value in the case of iodine while the reversed trend is apparent for the respective halogen atoms themselves upon descending from the lightest to the heaviest member of the group. The early onset of a negative charge for the carbon atom already in the CCl_3 group despite the still high difference in terms of electronegativity between carbon and chlorine could be attributed to the overall negative inductive effect of the halogen atoms that increases the "electron retaining" ability of the central carbon atom. It is pertinent to note that – as was observed for the carbon atoms of the aromatic scaffold – the natural charge of the oxygen atom also remains unaffected by the nature of the halogen atom present in the *ortho*-(trihalomethyl) group.

3.7 Bonding Situation

To assess the bonding situation in the homologous series of *ortho*-(trihalomethyl)phenols – especially with regard to the functional groups as well as the carbon atoms bearing the latter – NBO analyses were conducted. For all compounds it was invariably found that the contribution of the carbon atom to the C–O bond is above 33% although this figure slightly decreases with an increasing mass of the halogen atom present in the CX_3 group. A different picture is obtained examining the respective C–X bonds where the contribution of the carbon atom rises significantly with a decrease of the electronegativity of the halogen atom and spans a range of just 27% in the CF_3 group up to about 60% in the CI_3 group. Simultaneously, the p orbital contribution of the carbon atom increases as becomes apparent by its formal hybridization of $sp^{3.76}$ in the CF_3 group that grows to $sp^{4.01}$ in the CI_3 group. The natural electronic configuration of the carbon atom in the various *ortho*-(trihalomethyl)phenols is in agreement with the natural charges as discussed in the previous section as it increases from $s^{0.79}p^{2.08}$ for the fluorine derivative to $s^{1.26}p^{3.35}$ for the iodine derivative. If Rydberg orbitals as well as core-centered electrons are neglected, second order perturbation theory calculations invariably show the interaction of one of the lone pairs on the oxygen atom and the anti-bonding orbital of the C1–C2 bond (labelling according to Figure 4) to be the most stabilizing factor whose energy monotonously decreases from 125 kJ mol^{-1} for *ortho*-(trifluoromethyl)phenol to 120 kJ mol^{-1} for *ortho*-(triiodomethyl)phenol. If interactions between exclusively anti-bonding orbitals are included into the discussion, a much stronger pronounced trend is observed for the anti-bonding orbitals of the C1–C2 and the C5–C6 bond where a steady decrease in stabilization energy from 729 kJ mol^{-1} for the CF_3 derivative to 588 kJ mol^{-1} for the CI_3 derivative is calculated.

An inspection of the highest occupied molecular orbital (HOMO) and the lowest unoccupied molecular orbital (LUMO) shows the former to be centered on the trihalomethyl group for all four *ortho*-(trihalomethyl) phenols while the latter is located on the carbon and

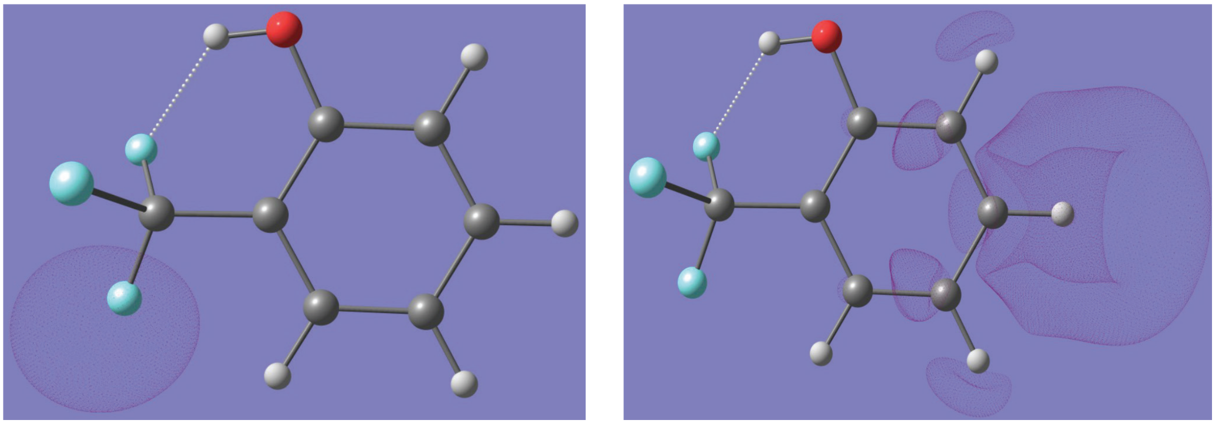

Figure 6: Isosurface plots of the highest occupied molecular orbital (HOMO) and the lowest unoccupied molecular orbital (LUMO) of *ortho*-(trifluoromethyl)phenol. Very similar pictures are obtained for the other *ortho*-(trihalomethyl)phenols.

hydrogen atoms in *meta*- and *para*-position to the respective trihalomethyl entities of the aromatic system. As an example, isocontour plots of the CF_3 derivative are shown in Figure 6.

The energetic gap between these two types of orbitals decreases with increasing mass of the halogen present in the CX_3 group – while a gap of 543 kJ mol^{-1} is found for *ortho*-(trifluoromethyl)phenol, this value drops in steps of approximately 70 kJ mol^{-1} for each heavier homologue of fluorine to, eventually, 334 kJ mol^{-1} in *ortho*-(triiodomethyl) phenol.

4 Conclusions

The crystal and molecular structure of commercially-available *ortho*-(trifluoromethyl)phenol were determined as the first example of an *ortho*-CX_3-substituted phenol derivative and found to be a defined hydrate in the crystalline state. An analysis of the hydrogen bonding system present in the title compound revealed parallels to the crystal structure of the hydrate of non-substituted phenol as well as the crystal structure of a high-pressure polymorph of anhydrous phenol. DFT calculations on the title compound as well as its higher homologues featuring the heavier halogens allowed for an assessment of the bonding situation as well as charge distribution on specific atoms of the individual compounds allowing for the identification of potential reaction sites for attacks of nucleophiles and electrophiles for further derivatization reactions. With this knowledge at hand, concise experimental studies about derivatives of the title compound as well as other *ortho*-(trihalomethyl) phenols can be conducted, not only with regard to their coordination behaviour to main group elements or transition metals but also with regards to further derivatization reactions starting from these materials. The unexpected and surprising presence of a molecule of water in the title compound (turning it into the half-hemi-hydrate) that was confirmed – although neither the compound's description nor the analytical certificate did specify it – explains the hydrolysis products observed upon reacting it with substrates prone to hydrolysis. This finding further reinforces the notion that one has to remain suspicious about the nature and identity of starting materials regardless of provider or date of purchase.

Acknowledgements: The author acknowledges financial support by Nelson Mandela Metropolitan University. The Center for High Performance Computing in Cape Town is thanked for generous allocation of calculation time.

Conflict of interest: Author states no conflict of interest.

References

[1] Weast R.C., CRC Handbook of Chemistry and Physics, 56th ed., CRC Press, Cleveland, 1975.
[2] Ballinger P., Long F.A., Acid Ionization Constants of Alcohols. II. Acidities of Some Substituted Methanols and Related Compounds, J. Am. Chem. Soc., 1960, 82, 795–798.
[3] Becker H.G.O., Beckert R., Domschke G., Fanghänel E., Habicher W.D., Metz P., Pavel D., Schwetlick K., Organikum, 21st ed., Wiley-VCH, Weinheim 2001.
[4] Arrowsmith M., Hill M.S., Kociok-Kohn G., MacDougall D.J., Mahon M.F., Mallov I., Three-Coordinate Beryllium

β-Diketiminates: Synthesis and Reduction Chemistry, Inorg. Chem., 2012, 51, 13408–13418.

[5] Cole M.L., Hibbs D.E., Jones C., Junk P.C., Smithies N.A., Imidazolium formation from the reaction of N-heterocyclic carbene stabilised group 13 trihydride complexes with organic acids, Inorg. Chim. Acta, 2005, 358, 102–108.

[6] van Poppel L.H., Bott S.G., Barron A.R., Molecular structures of Ga(^{t}Bu)$_2$(OPh)(pyz)·PhOH and [(^{t}Bu)$_2$Ga(H$_2$O)(μ-OH)Ga(^{t}Bu)$_2$]$_2$(μ-OC$_6$H$_4$O)·4(2-Mepy): intra- and inter-molecular hydrogen bonding to gallium aryloxides, Polyhedron, 2002, 21, 1877–1882.

[7] Linti G., Frey R., Polborn K., Zur Chemie des Galliums, IV. Darstellung und Strukturen monomerer (2,2,6,6-Tetramethylpiperidino)gallane, Chem. Ber., 1994, 127, 1387–1393.

[8] van Poppel L.H., Bott S.G., Barron A.R., 1,4-Dioxobenzene Compounds of Gallium: Reversible Binding of Pyridines to [{(^{t}Bu)$_2$Ga}$_2$(μ-OC$_6$H$_4$O)]$_n$ in the Solid State, J. Am. Chem. Soc., 2003, 125, 11006–11017.

[9] Chernov O.V., Smirnov A.Y., Portnyagin I.A., Khrustalev V.N., Nechaev M.S., Heteroleptic tin (II) dialkoxides stabilized by intramolecular coordination Sn(OCH$_2$CH$_2$NMe$_2$)(OR) (R=Me, Et, iPr, tBu, Ph). Synthesis, structure and catalytic activity in polyurethane synthesis, J. Organomet. Chem., 2009, 694, 3184–3189.

[10] Rocks S.S., Brennessel W.W., Machonkin T.E., Holland P.L., Solution and Structural Characterization of Iron(II) Complexes with Ortho-Halogenated Phenolates: Insights Into Potential Substrate Binding Modes in Hydroquinone Dioxygenases, Inorg. Chem., 2010, 49, 10914–10929.

[11] Tsai M.-C., Tsai F.-T., Lu T.-T., Tsai M.-L., Wie Y.-C., Hsu I.-J., Lee J.-F., Liaw W.-F., Relative Binding Affinity of Thiolate, Imidazolate, Phenoxide, and Nitrite Toward the {Fe(NO)$_2$} Motif of Dinitrosyl Iron Complexes (DNICs): The Characteristic Pre-Edge Energy of {Fe(NO)$_2$}^{9} DNICs, Inorg. Chem., 2009, 48, 9579–9591.

[12] Esteruelas M.A., Garcia-Raboso J., Olivan M., Preparation of Half-Sandwich Osmium Complexes by Deprotonation of Aromatic and Pro-aromatic Acids with a Hexahydride Brønsted Base, Organometallics, 2011, 30, 3844–3852.

[13] Edwards P.G., Andersen R.A., Zalkin A., Tertiary phosphine derivatives of the f-block metals. Preparation of X$_4$M(Me$_2$PCH$_2$CH$_2$PMe$_2$)$_2$, where X is halide, methyl or phenoxy and M is thorium or uranium. Crystal structure of tetraphenoxybis[bis(1,2-dimethylphosphino)ethane] uranium(IV), J. Am. Chem. Soc., 1981, 103, 7792–7794.

[14] Evans W.J., Miller K.A., DiPasquale A.G., Rheingold A.L., Stewart T.J., Bau R., A Crystallizable f-Element Tuck-In Complex: The Tuck-in Tuck-over Uranium Metallocene [(C$_5$Me$_5$)U{μ-η^5:η^1:η^1-C$_5$Me$_3$(CH$_2$)$_2$}(μ-H)$_2$U(C$_5$Me$_5$)$_2$], Angew. Chem., Int. Ed., 2008, 47, 5075–5078.

[15] Spirlet M.R., Rebizant J., Apostolidis C., van den Bossche G., Kanellakopulos B., Structure of tris(η^5-cyclopentadienyl) phenolatouranium(IV), Acta Crystallogr., Sect. C: Cryst. Struct. Commun., 1990, 46, 2318–2320.

[16] De Ridder D.J.A., Apostolidis C., Rebizant J., Kanellakopulos B., Maier R., Tris(η^5-cyclopentadienyl)phenolatoneptunium(IV), Acta Crystallogr., Sect. C: Cryst. Struct. Commun., 1996, 52, 1436–1438.

[17] Domingos A., Marcalo J., Pires de Matos A., Bis[hydrotris(pyrazolyl)borate] thorium(IV) complexes: Synthesis and characterization of alkyl, thiolate, alkoxide and aryloxide derivatives and the x-ray crystal structure of Th(HBPz$_3$)$_2$(OPh)$_2$, Polyhedron, 1992, 11, 909–915.

[18] Zadrozny J.M., Telser J., Long J.R., Slow magnetic relaxation in the tetrahedral cobalt(II) complexes [Co(EPh)$_4$]$^{2-}$ (EO, S, Se), Polyhedron, 2013, 64, 209–217.

[19] Howard W.A., Trnka T.M., Parkin G., Syntheses of the Phenylchalcogenolate Complexes (h^5-C$_5$Me$_5$)$_2$Zr(EPh)$_2$ (E = O, S, Se, Te) and (h^5-C$_5$H$_5$)$_2$Zr(OPh)$_2$: Structural Comparisons within a Series of Complexes Containing Zirconium-Chalcogen Single Bonds, Inorg. Chem., 1995, 34, 5900–5909.

[20] Evans W.J., Miller K.A., Ziller J.W., Synthesis of (O$_2$CEPh)$^{1-}$ Ligands (E = S, Se) by CO$_2$ Insertion into Lanthanide Chalcogen Bonds and Their Utility in Forming Crystallographically Characterizable Organoaluminum Complexes [Me$_2$Al(μ-O$_2$CEPh)]$_2$, Inorg. Chem., 2006, 45, 424–429.

[21] Hascall T., Murphy V.J., Parkin G., Reversible C–H Bond Activation in Coordinatively Unsaturated Molybdenum Aryloxy Complexes, Mo(PMe$_3$)$_4$(OAr)H: Comparison with Their Tungsten Analogs, Organometallics, 1996, 15, 3910–3912.

[22] Davies J.I., Gibson J.F., Skapski A.C., Wilkinson G., Wong W.-K., Synthesis of the hexaphenoxotungstate(V) ion; The x-ray crystal structures of the tetraethylammonium and lithium salts, Polyhedron, 1982, 1, 641–646.

[23] Lehtonen A., Sillanpaa R., Reactions of tris (1,2-ethanediolato) tungsten (VI) with phenyl acetates. X-ray structures of three products, Polyhedron, 1999, 18, 175–179.

[24] Boyle T.J., Pedrotty D.M., Alam T.M., Vick S.C., Rodriguez M.A., Structural Diversity in Solvated Lithium Aryloxides. Syntheses, Characterization, and Structures of [Li(OAr)(THF)$_x$]$_n$ and [Li(OAr)(py)$_x$]$_2$ Complexes Where OAr = OC$_6$H$_5$, OC$_6$H$_4$(2-Me), OC$_6$H$_3$(2,6-(Me))$_2$, OC$_6$H$_4$(2-Pri), OC$_6$H$_3$(2,6-(Pri))$_2$, OC$_6$H$_4$(2-But), OC$_6$H$_3$(2,6-(But))$_2$, Inorg. Chem., 2000, 39, 5133–5146.

[25] Moravec Z., Sluka R., Necas M., Jancik V., Pinkas J., A Structurally Diverse Series of Aluminum Chloride Alkoxides [Cl$_x$Al(μ-OR)$_y$]$_n$ (R = ^{n}Bu, ^{c}Hex, Ph, 2,4-^{t}Bu$_2$C$_6$H$_3$), Inorg. Chem., 2009, 48, 8106–8114.

[26] Cleaver W.M., Barron A.R., McGufey A.R., Bott S.G., Alcoholysis of tri-tert-butylgallium: synthesis and structural characterization of [(But)$_2$Ga(μ-OR)]$_2$, Polyhedron, 1994, 13, 2831–2846.

[27] Briand G.G., Decken A., McKelvey J.I., Zhou Y., Structural Effects of Varied Steric Bulk in 2,(4),6-Substituted Dimethylthallium(III) Phenoxides, Eur. J. Inorg. Chem., 2011, 2298–2305.

[28] Bortoluzzi M., Guazzelli N., Marchetti F., Pampaloni G., Zacchini S., Convenient synthesis of fluoride-alkoxides of Nb(V) and Ta(V): a spectroscopic, crystallographic and computational study, Dalton Trans., 2012, 41, 12898–12906.

[29] Yasuda H., Choi J.-C., Lee S.-C., Sakakura T., Structure of dialkyltin diaryloxides and their reactivity toward carbon dioxide and isocyanate, J. Organomet. Chem., 2002, 659, 133–141.

[30] Yeh S.-W., Lin C.-W., Li Y.-W., Hsu I.-J., Chen C.-H., Jang L.-Y., Lee J.-F., Liaw W.-F., Insight into the Dinuclear {Fe(NO)$_2$}^{10}{Fe(NO)$_2$}^{10} and Mononuclear {Fe(NO)$_2$}^{10} Dinitrosyliron Complexes, Inorg. Chem., 2012, 51, 4076–4087.

[31] Watenpaugh K., Caughlan C.N., The Crystal and Molecular Structure of Dichlorodiphenoxytitanium(IV), Inorg. Chem., 1966, 5, 1782–1786.

[32] Pasquali M., Fiaschi B., Floriani C., Manfredotti A.G., Bridging phenoxo-ligands in dicopper(I) complexes: synthesis and structure of tetrakis(isocyanide)-bis(μ-phenoxo)-dicopper(I) complexes, J. Chem. Soc., Chem. Commun., 1983, 197–199.

[33] Canty A.J., Devereux J.W., Skelton B.W., White A.H., Organo(organooxo)mercury(II) chemistry Synthesis and structure of methyl(phenoxo)mercury(II), Can. J. Chem., 2006, 84, 77–80.

[34] MacDougall D.J., Morris J.J., Noll B.C., Henderson K.W., Use of tetrameric cubane aggregates of lithium aryloxides as secondary building units in controlling network assembly, Chem. Commun., 2005, 456–458.

[35] Boersma J., Spek A.L., Noltes J.G., Coordination complexes of bis(2,2-dimethyl-3,5-hexanedionato) zinc with organozinc-oxygen and -nitrogen compounds. Crystal structure of the complex formed with phenylzinc phenoxide, J. Organomet. Chem., 1974, 81, 7–15.

[36] Enthaler S., Eckhardt B., Inoue S., Irran E., Driess M., Facile and Efficient Reduction of Ketones in the Presence of Zinc Catalysts Modified by Phenol Ligands, Chem. Asian J., 2010, 5, 2027–2035.

[37] Kunert M., Dinjus E., Nauck M., Sieler J., Structure and Reactivity of Sodium Phenoxide - Following the Course of the Kolbe-Schmitt Reaction, Chem. Ber., 1997, 130, 1461–1465.

[38] Watson K.A., Fortier S., Murchie M.P., Bovenkamp J.W., Crown ether complexes exhibiting unusual 1:2 macrocycle salt ratios: X-ray crystal structures of cyclohexano-15-crown-5•2LiOPh, cyclohexano-15-crown-5•2NaOPh, and 15-crown-5•2NaOPh, Can. J. Chem., 1991, 69, 687–695.

[39] Caulton K.G., Chisholm M.H., Drake S.R., Folting K., Synthesis and structural characterization of the first examples of molecular aggregates of barium supported by aryloxide and alkoxide ligands: $[HBa_5(O)(OPh)_9(thf)_8]$ and $[H_3Ba_6(O)(OBu^t)_{11}(OCEt_2CH_2O)(thf)_3]$(thf = tetrahydrofuran), J. Chem. Soc., Chem. Commun., 1990, 1349–1351.

[40] Malkowsky I.M., Frohlich R., Griesbach U., Putter H., Waldvogel S.R., Facile and Reliable Synthesis of Tetraphenoxyborates and Their Properties, Eur. J. Inorg. Chem., 2006, 1690–1697.

[41] Zozulin A.J., Moody D.C., Ryan R.R., Synthesis and structure of a mixed-valent uranium complex: tetra-m-phenoxy-di-m^3-oxo-bis(triphenoxy(tetrahydrofuran)uranium(V)) bis((tetrahydrofuran)dioxouranium(VI))], Inorg. Chem., 1982, 21, 3083–3086.

[42] Day V.W., Eberspacher T.A., Klemperor W.G., Liang S., Synthesis and Characterization of $BaTi(OC_6H_5)_6$•2DMF, a Single-Source Sol-Gel Precursor to $BaTiO_3$ Gels, Powders, and Thin Films, Chem. Mater., 1995, 7, 1607–1608.

[43] Drake S.R., Streib W.E., Chisholm M.H., Caulton K.G., Facile synthesis and structural principles of the strontium phenoxide $Sr_4(OPh)_8(PhOH)_2(THF)_6$, Inorg. Chem., 1990, 29, 2707–2708.

[44] Svetich G.W., Voge A.A., The crystal and molecular structure of *sym-trans*-di-μ-phenoxyhexaphenoxydiphenolatodititanium (IV), Acta Crystallogr., Sect. B: Struct. Crystallogr. Cryst. Chem., 1972, 28, 1760–1767.

[45] Gowda R.R., Chakraborty D., Ramkumar V., New Aryloxy and Benzyloxy Derivatives of Titanium as Catalysts for Bulk Ring-Opening Polymerization of ϵ-Caprolactone and δ-Valerolactone, Eur. J. Inorg. Chem., 2009, 2009, 2981–2993.

[46] Chandrasekaran A., Sood P., Day R.O., Holmes R.R., Chloro- and Fluoro-Substituted Phosphites, Phosphates, and Phosphoranes Exhibiting Sulfur and Oxygen Coordination, Inorg. Chem., 1999, 38, 3369–3376.

[47] Hopfl H., Hernandez J., Salas-Reyes M., Cruz-Sanchez S., Crystal structure of eq-2-p-trifluoromethylphenoxy-2-borane-cis-4,6- dimethyl-1,3,$2\lambda^3$-dioxaphosphorinane, $C_{12}H_{17}BF_3O_3P$, Z. Kristallogr. New Cryst. Struct., 2009, 224, 249–250.

[48] Theil I., Jiao H., Spannenberg A., Hapke M., Fine-Tuning the Reactivity and Stability by Systematic Ligand Variations in CpCoI Complexes as Catalysts for [2+2+2] Cycloaddition Reactions, Chem. Eur. J., 2013, 19, 2548–2554.

[49] Neu R.C., Ouyang E.Y., Geier S.J., Zhao X., Ramos A., Stephan D.W., Probing substituent effects on the activation of H2 by phosphorus and boron frustrated Lewis pairs, Dalton Trans., 2010, 39, 4285–4294.

[50] Kovacs A., Kolossvary I., Csonka G.I., Hargittai I., Theoretical study of intramolecular hydrogen bonding and molecular geometry of 2-trifluoromethylphenol, J. Comput. Chem., 1996, 17, 1804–1819.

[51] Gottlieb H.E., Kotlyar V., Nudelman A., NMR Chemical Shifts of Common Laboratory Solvents as Trace Impurities, J. Org. Chem., 1997, 62, 7512–7515.

[52] Frisch, M. J.; Trucks, G. W.; Schlegel, H. B.; Scuseria, G. E.; Robb, M. A.; Cheeseman, J. R.; Scalmani, G.; Barone, V.; Mennucci, B.; Petersson, G. A.; Nakatsuji, H.; Caricato, M.; Li, X.; Hratchian, H. P.; Izmaylov, A. F.; Bloino, J.; Zheng, G.; Sonnenberg, J. L.; Hada, M.; Ehara, M.; Toyota, K.; Fukuda, R.; Hasegawa, J.; Ishida, M.; Nakajima, T.; Honda, Y.; Kitao, O.; Nakai, H.; Vreven, T.; Montgomery, J. A., Jr.; Peralta, J. E.; Ogliaro, F.; Bearpark, M.; Heyd, J. J.; Brothers, E.; Kudin, K. N.; Staroverov, V. N.; Kobayashi, R.; Normand, J.; Raghavachari, K.; Rendell, A.; Burant, J. C.; Iyengar, S. S.; Tomasi, J.; Cossi, M.; Rega, N.; Millam, J. M.; Klene, M.; Knox, J. E.; Cross, J. B.; Bakken, V.; Adamo, C.; Jaramillo, J.; Gomperts, R.; Stratmann, R. E.; Yazyev, O.; Austin, A. J.; Cammi, R.; Pomelli, C.; Ochterski, J. W.; Martin, R. L.; Morokuma, K.; Zakrzewski, V. G.; Voth, G. A.; Salvador, P.; Dannenberg, J. J.; Dapprich, S.; Daniels, A. D.; Farkas, Ö.; Foresman, J. B.; Ortiz, J. V.; Cioslowski, J.; Fox, D. J., *Gaussian 09, Revision 01*, Gaussian Inc., Wallingford CT, 2009.

[53] Dennington, R.; Keith, T.; Millam, *GaussView*, J. Semichem Inc., Shawnee Mission KS, 2009.

[54] Wolinski K., Hinton J.F., Pulay P., Efficient implementation of the gauge-independent atomic orbital method for NMR chemical shift calculations, J. Am. Chem. Soc., 1990, 112, 8251–8260.

[55] Hanwell M.D., Curtis D.E., Lonie D.C., Vandermeersch T., Zurek E., Hutchison G.R., Avogadro: an advanced semantic chemical editor, visualization, and analysis platform, J. Cheminf. 2012, 4:17.

[56] Zhurko, G. A.; *Chemcraft* (Version 1.7, build 132). http://www.chemcraftprog.com.

[57] Sheldrick G.M., A short history of *SHELX*, Acta Crystallogr., Sect. A: Found. Crystallogr., 2008, 64, 112–122.

[58] Spek A.L., Structure validation in chemical crystallography, Acta Crystallogr., Sect. D: Biol. Crystallogr., 2009, 65, 148–155.

[59] Macrae C.F., Bruno I.J., Chisholm J.A., Edgington P.R., McCabe P., Pidcock E., Rodriguez-Monge L., Taylor R., van de Streek J., Wood P.A., *Mercury CSD 2.0* – new features for the visualization

and investigation of crystal structures, J. Appl. Crystallogr., 2008, 41, 466–470.

[60] Farrugia L.J., *WinGX* and *ORTEP for Windows*: an update, J. Appl. Crystallogr., 2012, 45, 849–854.

[61] Bernstein J., Davis R.E., Shimoni L., Chang N.-L., Patterns in Hydrogen Bonding: Functionality and Graph Set Analysis in Crystals, Angew. Chem. Int. Ed. Engl., 1995, 34, 1555–1573.

[62] Etter M.C., MacDonald J.C., Bernstein J., Graph-set analysis of hydrogen-bond patterns in organic crystals, Acta Crystallogr., Sect. B: Struct. Sci. 1990, 46, 256–262.

[63] Meuthen B., von Stackelberg M., Röntgenographische Untersuchungen an Dimethylphenolen, Z. Elektrochem., 1960, 64, 386–387.

[64] Allen F.H., The Cambridge Structural Database: a quarter of a million crystal structures and rising, Acta Crystallogr. Sect. B: Struct. Sci., 2002, 58, 380–388.

[65] Zavodnik V.E., Bel'skii V.K., Zorki P.M., <title unknown>, Zh. Strukt. Khim., 1987, 28, 175-5.

[66] Allan D.R., Clark S.J., Dawson A., McGregor P.A., Parsons S., Pressure-induced polymorphism in phenol, Acta. Crystallogr. Sect B: Struct. Sci., 2002, 58, 1018–1024.

[67] Hosten E.C., Betz R., Synthesis, spectral, and structural characteristics of cyanohydrines derived from aliphatic cyclic ketones, Russ. J. Gen. Chem., 2014, 84, 2222–2227.

[68] Bertolotti F., Gervasio G., Crystal structure of iodoform at 106K and of the adduct $CHI_3 \cdot 3(C_9H_7N)$. Iodoform as a building block of co-crystals, J. Mol. Struct., 2013, 1036, 305–310.

[69] Pohl S., Die Kristallstruktur von CI_4, Z. Kristallogr., Kristallgeom., Kristallphys., Kristallchem., 1982, 159, 211–216.

[70] Krossing I., Bihlmeier A., Raabe I., Trapp N., Structure and Characterization of $CI_3^+[Al\{OC(CF_3)_3\}_4]^-$; Lewis Acidities of CX_3^+ and BX_3, Angew. Chem., Int. Ed., 2003, 42, 1531–1534.

[71] Allen L.C., Electronegativity is the average one-electron energy of the valence-shell electrons in ground-state free atoms, J. Am. Chem. Soc., 1989, 111, 9003–9014.